DOI: 10.1002/chem.200701339

Simulations of *p-tert*-Butylcalix[4]arene with Multiple Occupancies of Small Guest Molecules

Saman Alavi* and John A. Ripmeester[a]

Abstract: Classical molecular dynamics simulations were used to study low-density β_0-phase *p-tert*-butylcalix[4]arene inclusion compounds with multiple calix occupancies of xenon, carbon dioxide, methane, and hydrogen guest molecules with guest–host ratios ranging from 1:4 to 4:1. Custom parameterized force fields were used for the guests and the AMBER force field for the calixarene units was validated in our previous work (*Chem. Eur. J.* **2006**, *12*, 5231). The inclusion energy and unit cell volume of the calixarene inclusion compound were determined for various guest occupancies and for occupancies greater than 1:1, strong guest–guest interaction effects are observed. The structure and energetics of the 2:1 CO_2/β_0-phase inclusion compound were compared to those of the low-temperature 2:1 CO_2/calixarene in which the guest molecules occupy both cage and interstitial sites.

Keywords: calixarenes · host–guest systems · inclusion compounds · molecular dynamics · multiple occupancy

Introduction

The pure form of the low-density β_0-phase of solid *p-tert*-butylcalix[4]arene (tBC) (Figure 1) crystallizes in the monoclinic $P2_1/n$ space group.[1,2] The β_0-phase is metastable at room temperature and has a density of 1.050 g cm^{-3}.[2] When exposed to low pressures of small gas-phase molecules such as Xe, NO, SO_2, N_2, O_2, H_2, and CO_2, the β_0-phase forms inclusion compounds in which the host lattice structure retains the $P2_1/n$ space group.[3,4] Upon heating the inclusion compound, the guest molecules are desorbed at temperatures that depend on the nature of the gas guest species. This variable retention of different gas-phase guest molecules can potentially be used for gas-phase separations.

A number of simulation studies of the interactions of guest molecules with the calixarene solid host lattice phases have appeared in the literature. Ogden and co-workers[5] used ab initio molecular dynamics calculations to study the host–guest interactions for CS_2 and toluene p-*tert*-butylcalix[4]rene inclusion compounds in the solid phase and for isolated gas-phase complexes. They observed that crystal packing has a significant effect on host–guest packing in the calixarenes. The predicted packing configurations of the guests in the crystal were in good agreement with experimentally determined structures for these compounds. León, Leigh, and Zerbetto[6] performed a molecular mechanics calculation with the MM3 force field on the effect of guest inclusion on crystal packing of the p-*tert*-butylcalix[4]arene solid. They studied a range of possible structural motifs observed for the self-included calixarenes and calixarene–guest complexes. They calculated small interaction energies between the guest and host (<30 kcal mol^{-1}) and predicted that the guest would be mobile in *endo*-calixarene complexes. The selectivity of isolated *p-tert*-butylcalix[4]arene molecules towards different guest molecules was studied by Daschbach et al.[7] using the potential of mean force method. Their study suggested that selective interactions of the calixarenes can be used for the separation of components of a gas mixture.

We have recently studied structural and dynamical behavior of β_0-phase calixarene inclusion compounds with xenon, nitrogen, hydrogen, methane, and SO_2 using molecular dynamics simulations[8] with guest–host occupancy ratios up to 1:1. At these occupancy ratios, the unit cell volume and inclusion energy were determined to vary linearly with guest occupancy and the guest molecules in adjacent calixes do not interact and adsorption is consistent with the Langmuir adsorption isotherm. The calculated inclusion energy of the guest molecules was found to correlate well with the temperature of release of the guests in the thermogravimetric experiment.[3]

[a] Dr. S. Alavi, Prof. J. A. Ripmeester
Steacie Institute for Molecular Sciences
National Research Council of Canada
100 Sussex Dr., Ottawa, Ontario K1A 0R6 (Canada)
Fax: (+1) 613-947-2838
E-mail: saman.alavi@nrc-nrc.gc.ca

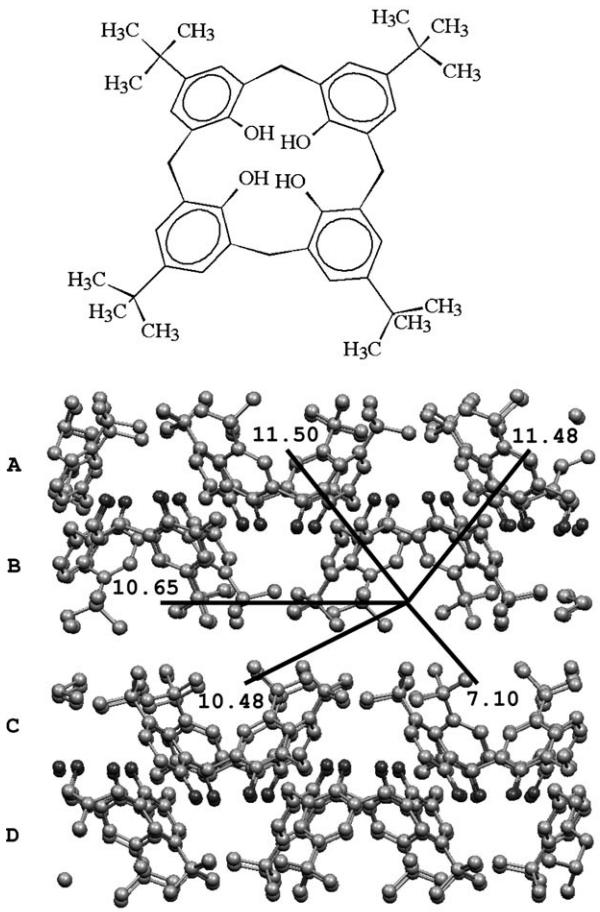

Figure 1. The structure of the *p-tert*-butylcalix[4]arene molecule (top) and the low-density calixarene β_0-phase. The four-layer ABCD repeat unit of the solid phase is shown along with characteristic distances between the centers of neighboring cages (in Ångstroms). Oxygen atoms are shown in black and carbon atoms in gray. For clarity, the hydrogen atoms are not shown.

The pressure and temperature of the formation of the inclusion compounds of xenon, carbon dioxide, methane, and hydrogen guests with less than 1:1 host–guest ratios along with the observed percent occupancy of the calixarenes are given in Table 1. In this work we study multiple occupancies of these guest molecules in the calixarenes with molecular dynamics simulations. The effects of multiple occupancies on the unit cell volume and inclusion energy are determined, and the radial distribution functions for the guest molecules in the multiple occupancy case are compared to those for the singly occupied cages. The doubly occupied carbon dioxide/β_0-phase calixarene is compared with the high-pressure 2:1 carbon dioxide/calixarene complex with interstitial guest molecules that has recently been experimentally observed at 125 K.[9] Alternative solid-state phases have also been recently observed for xenon tBC inclusion compounds for loadings greater than 0.25 for the host/guest ratio.[10] The formation of these alternative crystal structures is discussed in the context of the inclusion energies obtained for the tBC complexes.

Table 1. Experimental loading conditions for hydrogen, methane, carbon dioxide, and xenon guests in the low-density β_0-phase calixarene and mole percent of host calixarene occupancy.

Guest	*P* [atm]	*T* [K]	Host occupancy [%]
H_2[a]	31	298	66
CH_4[b]	35	298	71
CO_2[c]	1	296	40
CO_2[d]	300	313	80
Xe[e]	1	298	30

[a] Ref. [21]. [b] Ref. [22]. [c] Ref. [29]. [d] Ref. [28]. [e] Ref.[10].

Computational Methods

A $2\times2\times2$ replica of the unit cell of the low-density calixarene β_0-phase with $25.272\times51.538\times25.292$ Å^3 dimensions was used in the simulation; the positions of the atoms in the unit cell were taken from X-ray crystallographic data.[3] In the molecular dynamics simulations the *p-tert*-butylcalix[4]arene molecules are considered to be rigid, with intermolecular potentials considered to be a sum of Lennard-Jones (LJ) and electrostatic point charge potentials between atoms on different molecules:

$$V_{\text{inter}} = \sum_{i=1}^{N-1}\sum_{j>i=1}^{N}\left\{4\varepsilon_{ij}\left[\left(\frac{\sigma_{ij}}{r_{ij}}\right)^{12}-\left(\frac{\sigma_{ij}}{r_{ij}}\right)^{6}\right]+\frac{q_i q_j}{4\pi\varepsilon_0 r_{ij}}\right\} \qquad (1)$$

The LJ parameters ε_{ii} and σ_{ii} for the atoms of the calixarene cages were taken from the AMBER force field[11] and standard combination rules were used for the LJ potential parameters between unlike atom-type force centers i and j. Electrostatic point charges, q_i, on atoms of tBC were calculated from Mulliken analysis by using HF/6–31G(d) level calculations. The complete set of LJ parameters, electrostatic point charges, and Cartesian coordinates of the tBC molecules and details of the force fields for the xenon and methane guests are also given in reference [8]. The H_2 LJ parameters are taken from the Wang potential[12] with atomic point charges assigned to reproduce the gas-phase quadrupole moment of H_2. Carbon dioxide LJ parameters are taken from the elementary physical model (EPM) of Harris and Yung,[13] which was used in simulations of dense fluid carbon dioxide. Point charges on CO_2 were determined to reproduce the experimental gas-phase quadrupole moment of 4.3 Buckingham.[14] The LJ parameters and point charges of the guest molecules are given in Table 2.

Equilibrium properties of the inclusion compounds were calculated with isotropic NPT molecular dynamics simulations using the Nosé–Hoover thermostat–barostat algorithm[15–17] on the simulation cell with the DL_POLY 2.16.[18] The relaxation times for the thermostat and barostat were chosen as 0.1 and 1.0 ps, respectively. The equations of motion were integrated with a time step of 0.5 fs using the Verlet leapfrog scheme.[19,20] Coulombic long-range interac-

Table 2. Average atomic charges and Lennard-Jones interaction parameters used for the xenon, carbon dioxide, methane, and hydrogen guests in the MD simulations.

Atom	q [e]	σ_{ii} [Å]	ε_{ii} [kcal mol^{-1}]
Xe	0.0000	4.099	1.8480
C (in CO_2)	+0.6645	3.064	0.0576
O (in CO_2)	−0.33225	2.785	0.1649
C (in CH_4)	−0.572	3.350	0.1017
H (in CH_4)	+0.143	2.610	0.0171
H (in H_2)	+0.4932	2.68224	0.0288
H(cm) (in H_2)	−0.9864	0.000	0.0000

tions were calculated by using Ewald sums[19,20] with a precision of 1×10^{-6}, and all interatomic interactions in the simulation box were calculated within a cutoff distance of $R_{cutoff}=12.0$ Å. The simulations were carried out for a total time of 100 ps, in which the first 10 ps were used for temperature scaled equilibration. For CO_2, CH_4, and Xe, occupancies up to two guests per calixarene molecule, and for the smaller H_2 guests, occupancies up to four were considered. The simulations were carried out at a pressure of 1.013 bar and a temperature of 173 K.

The experimental crystal structure for a tetragonal high-pressure 2:1 CO_2/host calixarene at 125 K has been determined[9] for which one CO_2 guest occupies a calixarene cage and the second CO_2 molecule resides in an interstitial site and is aligned along the unit cell c axis. The unit cell of this phase is shown in Figure 2. We will compare the unit cell volume and inclusion energy for this phase with the hypothetical doubly occupied low-density β_0-phase calixarene. A $2\times2\times4$ replica of the unit cell of this high-pressure phase with $25.442\times25.442\times50.340$ Å^3 dimensions was used in the simulations.

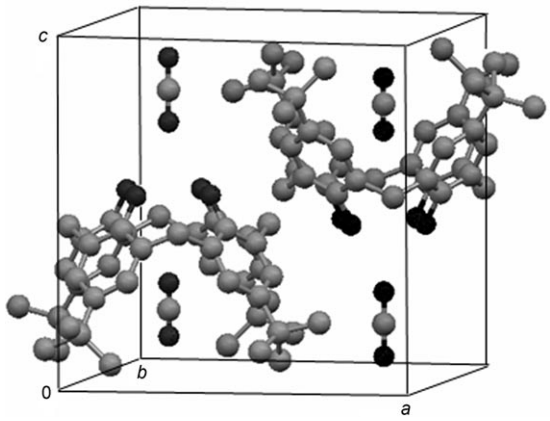

Figure 2. The unit cell structure of the interstitial phase of the 2:1 CO_2-*p*-*tert*-butylcalix[4]arene inclusion compound. The structural data is taken from reference [9]. Oxygen atoms are shown in black and carbon atoms in gray. For clarity, the hydrogen atoms are not shown.

Results and Discussion

The H_2–H_2 center-of-mass, CH_4–CH_4 carbon–carbon, CO_2–CO_2 carbon–carbon, and Xe–Xe radial distribution functions (RDFs) at a pressure of 1.013 bar and a temperature of 173 K for the multiply occupied guest–host solids are shown in Figures 3 to 6, respectively. In each Figure, the LJ interaction potential (in arbitrary energy units) for the guest–guest interactions is given for reference.

The adsorption of H_2 gas to the extent of 0.2 wt% was measured for tBC at room temperature and 31.0 atm equilibrium pressure.[21] This roughly corresponds to a 2/3 occupancy of the calixarene bowls. The RDFs for the H_2–tBC inclusion compounds with guest–host ratios of 1:1 to 4:1 are shown in Figure 3. The maximum of the first broad peak in

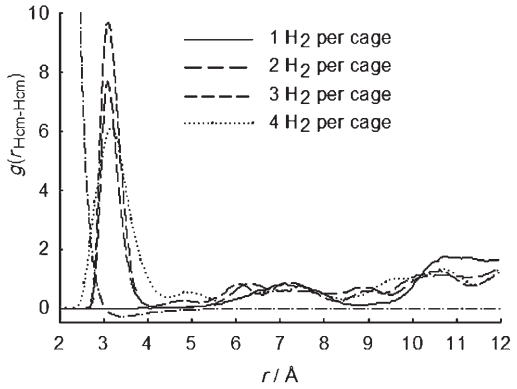

Figure 3. The hydrogen–hydrogen center-of-mass radial distribution functions for the fully occupied 1:1, 2:1, 3:1, and 4:1 guest–host calixarene for the 173 K simulation at 1.013 bar. The H_2–H_2 Lennard-Jones potential is shown with the dot-dash line to characterize the guest–guest interactions. The scale of the y axis of the LJ potential is arbitrary.

the RDF for the singly occupied H_2 inclusion compound lies near 7 Å and corresponds to the separation of hydrogen molecules from paired calixarenes in facing rows shown in Figure 1. The next broad peak in the singly occupied cages starts near 10.5 Å and corresponds to the separations of guests from the next nearest neighboring calixarenes from the facing rows in Figure 1. The doubly to quadruply occupied H_2–calixarenes show a sharp peak in the RDF at a separation of about 3 Å. This average separation of hydrogen molecules in the guest cluster corresponds to a bulk density of 0.03 g cm^{-3}. For comparison, the density of liquid hydrogen at its boiling point of 20 K at atmospheric pressure is 0.07 g cm^{-3}. The broad peaks of the RDFs indicate guest motions in the cages.

An equilibrium methane–tBC inclusion compound saturated with 1.7 wt% methane forms at a methane pressure of 35 atm, at room temperature (starting from an initial pressure of 38 atm). Full occupancy of all bowls with methane corresponds to 2.4 wt% methane.[22] Starting with lower initial pressures of methane, equilibrium was attained at a pressure of 410 Torr, and the molar ratio of methane to calixarene was determined to be 14%.[22–24] Only diffuse electronic density data could be obtained from single-crystal X-ray diffraction data of the methane–tBC inclusion compound. The solid-state NMR spectrum revealed a ^{13}C resonance at $\delta=-11.3$ ppm for the guest methane in the calixar-

ene.[24] This shift can be compared to ^{13}C methane resonances ranging from $\delta = -8$ ppm in zeolites,[25] $\delta = -9.4$ ppm in tris-o-phenylenedioxycyclotriphosphazine,[26] and $\delta = -4$ ppm observed for methane clathrates.[27] This large upfield shift implies relatively strong interactions of the methane with the ring currents in the calix. Evidence of methane diffusion through the cages was observed.[23] The first maximum of the singly occupied CH_4–calixarene carbon–carbon RDFs (shown in Figure 4) is calculated to be about 6.8 Å,

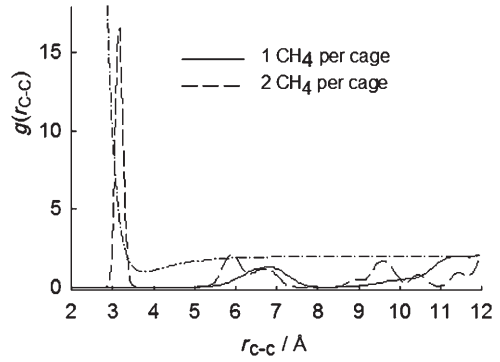

Figure 4. The CH_4–CH_4 center-of-mass radial distribution functions for the fully occupied 1:1 and 2:1 guest–host calixarene for the 173 K simulation at 1.013 bar. The CH_4–CH_4 Lennard-Jones potential is shown with the dot-dash line to characterize the guest–guest interactions. The scale of the *y* axis of the LJ potential is arbitrary.

and for the doubly occupied inclusion compound the CH_4 guests in the same cage display a peak in the RDF at a distance of about 3.2 Å. In the doubly occupied case, the first CH_4 RDF peak lies mostly in the repulsive region of the LJ carbon-carbon interaction potential, and a repulsive energy contribution from placing a second CH_4 molecule in the calixarene cage is expected.

The formation of the inclusion compound of CO_2 in tBC was observed with solid-state NMR spectroscopy by Graham et al.[28] at 40 °C and 30 MPa CO_2 (supercritical) pressure. The ^{13}C peak for CO_2 in the inclusion compound was observed at $\delta = 129.9$ ppm. X-ray structure data could not be obtained from these crystals of this inclusion compound, and thermogravimetric analysis showed that under these conditions, 70% of the tBC molecules incorporated a CO_2 guest.[28] Atwood and co-workers[4,29] state a CO_2 occupancy of 80% in the cavities (two host molecules) at atmospheric pressure and 23 °C, and they reported a ^{13}C NMR signal for CO_2 at $\delta = 121.9$ ppm. In a recent experiment, Udachin et al.[9] were able to obtain single-crystal X-ray structural data for the 1:1 and 2:1 CO_2/tBC compounds. In the 1:1 compound, the CO_2 molecules located inside the calix gave rise to an average angle of 26.6° with respect to the pseudo-fourth order axis of the calix. In the 2:1 calixarene, the interstitial CO_2 molecules lie along the fourfold symmetry axis of the calix, whereas the guest molecules in the calix are tilted at an average angle of 35.4° with respect to this axis. The closest O–O distance between the CO_2 guests in the 2:1 compound was determined to be 2.8 Å. The ^{13}C NMR chemical shift of the CO_2 carbon in the 1:1 compound was determined to be $\delta = 122.4$ ppm. The 2:1 calixarene displays a single line in the ^{13}C spectrum with a measured chemical shift of $\delta = 123.6$ ppm. The single line in the NMR spectrum of the 2:1 calixarene shows that the interstitial CO_2 guest and the guest in the calix undergo a rapid exchange.

In the singly occupied inclusion compound, the first maximum of the CO_2 carbon–carbon RDFs (Figure 5) is calculat-

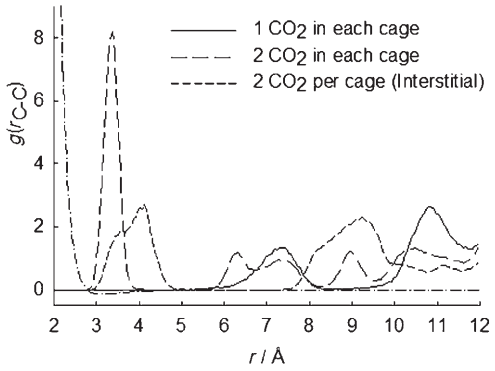

Figure 5. The CO_2–CO_2 center-of-mass radial distribution functions for the fully occupied 1:1 and 2:1 guest–host calixarene for the 173 K simulation at 1.013 bar. The RDF of the high-pressure CO_2 calixarene is also included for comparison. The CO_2–CO_2 Lennard-Jones potential is shown with the dot-dash line to characterize the guest–guest interactions. The scale of the *y* axis of the LJ potential is arbitrary.

ed to be at about 7.3 Å which corresponds to the random distribution of the CO_2 molecules in adjacent calixarene cages. With double occupancy in the β_0 framework, the two CO_2 guests in the same cage display a peak in the RDF at a distance of about 3.2 Å. The interstitial 2:1 guest–host inclusion compound shown in Figure 2 has a broad first peak at about 4.0 Å with a shoulder at about 3.4 Å. The interstitial complex allows larger separations between the CO_2 guests.

Experiments show that for host–guest ratios less than 0.25, the solid-state phase of the Xe–calixarene inclusion compound maintains the $P2_1/n$ space group and unit cell vectors of the β_0-phase.[10] For host–guest ratios of 0.25, the separations of xenon atoms from X-ray crystallography in the 0.25 occupied inclusion compound are 6.78 and 10.39 Å, respectively,[10] and from ^{129}Xe–^{129}Xe dipolar coupling in double quantum (DQ) NMR spectra[10] the Xe–Xe distance is determined to be 6.6 Å. In the simulations, for xenon occupations up to 1:1, the first maximum in the RDF, shown in Figure 6, lies between 6 and 7 Å, and the broad peak in the RDF between 9 and 10.5 Å corresponds to the separation of xenon atoms from the next nearest neighboring calixarenes in the lattice. These values are in excellent agreement with the experimental values. The calculated first Xe–Xe separation is somewhat smaller than the other nearest guest–guest separations studied in this work.

In the doubly occupied xenon inclusion compound the first large maximum in the RDF lies at about 4.5 Å and represents two xenon atoms in the same calixarene bowl. The

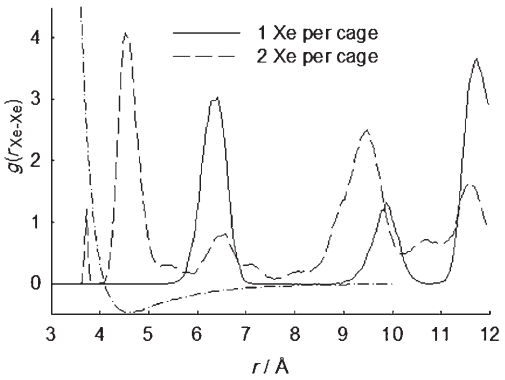

Figure 6. The xenon–xenon radial distribution functions for the 1:1 and 2:1 guest–host calixarene for the 173 K simulation at 1.013 bar. The Xe–Xe Lennard-Jones potential is shown with the dot-dash line to characterize the guest–guest interactions. The scale of the *y* axis of the LJ potential is arbitrary.

separation of these two guests corresponds to the minimum of the Xe−Xe LJ interaction potential, but a comparison of the width of the RDF peak with the LJ interaction potential shows that there is a significant repulsive component to the interactions for Xe–Xe pairs in the same calixarene cage. Experimentally, at guest–host ratios greater than 0.25, a second peak arises in the ^{129}Xe NMR spectrum which has been interpreted as being related to a new configuration with closest Xe−Xe separations at 8.8 Å.[10] Our simulation results agree with other experimental evidence[10] that these second peaks do not represent doubly occupied calixarene cages and are caused by a solid-state phase transition that arises from the sliding of adjacent calixarene layers.

The inclusion energy per unit cell, ΔE_{incl}, for the guest molecules is defined by Equation (2):

$$\Delta E_{incl} = E(\text{guest-calix}) - E(\text{calix}) - E(\text{guest}) \quad (2)$$

where E(guest-calix) and E(calix) are the energies per unit cell of the guest-calixarene solid phase at each occupancy and the pure β_0-phase calixarene, respectively. The free guests molecules are assumed to be ideal gases with energies, $E(\text{guest}) = 3nRT/2$, where n is the moles of guest molecules per unit cell and R is the gas constant. This assumes the guest molecules have the same rotational energy in the calixarene phase as free gas molecules. The inclusion energies for different occupancies of the H_2, CH_4, CO_2, and Xe guests are given in Table 3 and plotted in Figure 7. The linear variation of the inclusion energy for occupancies up to 1:1 shows that within the scope of the present simulations, guests in singly occupied adjacent adsorption sites do not appreciably interact and the Langmuir adsorption isotherm can be valid for describing the adsorption process. Using the values in Table 3, for the 1:1 guest-to-host ratio, the inclusion energy per guest for xenon is the largest at −24.0 kcal mol^{-1}, followed by CO_2 with −10.2 kcal mol^{-1}, and methane and hydrogen guests with −6.7 kcal mol^{-1} and −2.2 kcal mol^{-1}, respectively. The values of the inclusion

Table 3. Dependence of the calculated inclusion energy per unit cell (kcal mol^{-1}) with occupation fraction for xenon, carbon dioxide, methane, and hydrogen guests in the low-density β_0-phase calixarene at 173 K and 1.013 bar pressure. The error bars in the energies are 0.5 kcal mol^{-1}.

Occupation	ΔE_{incl}(Xe)	ΔE_{incl}(CO_2)	ΔE_{incl}(CH_4)	ΔE_{incl}(H_2)
0.25	−24.4	−10.5	−6.2	−2.2
0.50	−47.8	−21.1	−13.9	−4.8
0.75	−71.7	−30.8	−20.5	−6.7
1.00	−95.9	−40.8	−26.9	−9.0
1.50	−51.0			
2.00	−89.1	−60.3	−29.8	−13.3
3.00			−16.1	
4.00			−17.9	

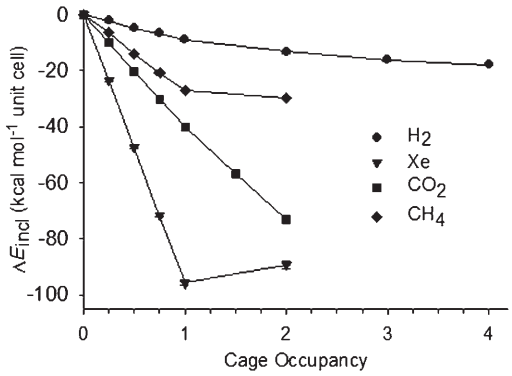

Figure 7. The variation of the inclusion energy per unit cell (kcal mol^{-1}) for *p-tert*-butylcalix[4]arene with xenon, carbon dioxide, methane, and hydrogen guest occupancies for the 173 K simulation at 1.013 bar. For occupancies greater than 1:1, deviations from linearity are observed.

energy give an indication of the conditions required to maintain the stability of the calixarene compound as given in Table 1. It can be seen that the H_2 and CH_4 guests that have the smallest inclusion energies require the highest pressures to maintain their stability.

For the 2:1 inclusion compounds, the repulsive interactions between guests in the same cages contribute to a decrease in the magnitude of the inclusion energy as compared to the 1:1 compounds. This trend is particularly noticeable in the inclusion energy of the xenon and methane clathrate since repulsive interactions among guests in the same calixarene cage can be large, see Figure 4 and 6. Deviations from linearity in the inclusion energy/occupancy curves are seen for all guests, implying that a simple Langmuir isotherm will not apply over the range of occupancies greater than 1:1.

The dependence of the unit cell volume and density on the fractional guest occupancy at 173 K and ambient pressure are given in Table 4 and the unit cell volumes are shown in Figure 8. In Figure 8, it is seen that up to an occupancy ratio of 1:1, the addition of xenon guests to the calixarene causes a decrease in the unit cell volume. The repulsion among the two xenon guests in the 2:1 guest–host compound causes an increase in the unit cell volume of about 15%, which is outside the scale of this Figure. For the other guests, the increase in the unit cell volume upon reaching 1:1 occupancy is negligible. A roughly 2% volume increase

Table 4. Dependence of the calculated unit cell volume and density with the occupation fraction for xenon, carbon dioxide, methane, and hydrogen guests in low-density β_0-phase calixarene at 173 K and 1.013 bar pressure. The error in the density values is 0.003 gcm^{-3}.

Occupation	V_{calcd} [Å^3]	ρ_{calcd} [g cm^{-3}]	
	0.00	3903.3 ± 9.1	1.104
Xe	0.25	3894.4 ± 10.1	1.163
	0.50	3886.0 ± 8.8	1.221
	0.75	3878.6 ± 8.0	1.280
	1.00	3870.4 ± 8.2	1.339
	2.00	4552.2 ± 14.5	1.330
CO_2	0.25	3900.4 ± 10.5	1.124
	0.50	3899.2 ± 9.4	1.143
	0.75	3896.5 ± 10.0	1.162
	1.00	3893.9 ± 9.4	1.182
	1.50	3924.9 ± 10.0	1.210
	2.00	3947.4 ± 9.6	1.240
		3912.0 ± 8.5[a]	1.251[a]
CH_4	0.25	3989.4 ± 8.9	1.112
	0.50	3897.4 ± 7.9	1.120
	0.75	3894.8 ± 10.1	1.127
	1.00	3893.0 ± 8.9	1.134
	2.00	3943.9 ± 9.2	1.147
H_2	0.25	3902.1 ± 8.4	1.105
	0.50	3901.1 ± 8.5	1.106
	0.75	3901.8 ± 9.2	1.107
	1.00	3899.1 ± 9.5	1.109
	2.00	3904.6 ± 8.5	1.111
	3.00	3922.2 ± 9.5	1.109
	4.00	3930.4 ± 10.0	1.110

[a] Determined from experiment for interstitial CO_2 phase described in reference [9].

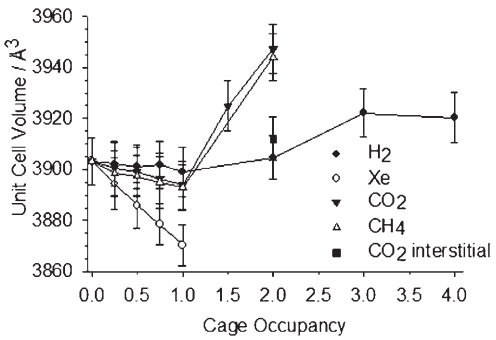

Figure 8. The variation of the unit cell volume (Å^3) for *p-tert*-butylcalix[4]arene with xenon, carbon dioxide, and methane for 1:4 to 2:1 guest/host complexes, and hydrogen for 1:4 to 4:1 guest/host complexes for the 173 K simulation at 1.013 bar. The unit cell volume of the interstitial 2:1 guest/host carbon dioxide complex is also show. The unit cell volume of the 2:1 Xe inclusion compound is out of the range of this Figure and is not shown.

for CO_2– and CH_4–calixarenes is observed upon reaching double occupancy. The volume of the interstitial 2:1 CO_2–calixarene shown in Figure 8 is significantly lower than the hypothetical 2:1 calixarene studied in this work.

For xenon occupancies greater than 0.25 the adjacent layers of tBC cages rearrange in a manner that retains the existing single-crystal structure.[10] Due to the strong restraints of periodic boundary conditions, these rearrangements are difficult to reproduce in MD calculations. Experimentally, inclusion of the second CO_2 guest molecule in the calixarene leads to the formation of a solid-state phase with both intercalixarene and interstitial guest molecules.[9] The common characteristic of the Xe– and CO_2–tBC inclusion compounds is the large inclusion energies for the guests. These large inclusion energies can affect the balance of the energies that determine the solid-state structure and lead to phase transitions at higher guest ratios. The H_2 and CH_4 guests with small inclusion energies are not expected to cause phase transitions in the calixarene solid phase.

Conclusion

Molecular dynamics simulations were used to study calixarene inclusion compounds with xenon, carbon dioxide, methane, and hydrogen guest molecules. The AMBER force field is used for the intermolecular Lennard-Jones interaction parameters of the calixarenes and specialized force fields are used for the guests in the simulations.

The unit cell volume and inclusion energy, defined in Equation (2) for different guest/host ratios are determined in this work. Up to a host/guest ratio of 1:1, these quantities show linear variation with guest occupancy which implies the absence guest–guest interactions in neighboring cages. The inclusion energies of xenon, carbon dioxide, methane, and hydrogen are −24.0, −10.2, −6.7, and −2.2 kcal mol^{-1}, respectively.

The Xe– and CO_2–tBC inclusion compounds are experimentally observed to exhibit solid-state phase transitions at occupancy ratios greater than 0.25 and 1, respectively. These two guests have the largest inclusion energies in the calixarene. The large inclusion energies can affect the balance of forces in the clathrate structure and lead to different calixarene solid-state structures. The magnitude of the calculated inclusion energy in the β_0-phase may be used as an indication of whether solid-state phase transitions are likely to occur in the inclusion compounds.

Acknowledgement

This work was supported by the National Research Council of Canada.

[1] E. B. Brouwer, G. D. Enright, K. A. Udachin, S. Lang, K. J. Ooms, P. A. Halchuk, J. A. Ripmeester, *Chem. Commun.* **2003**, 1416–1417.
[2] J. L. Atwood, L. J. Barbour, A. Jerga, B. L. Schottel, *Science* **2002**, *298*, 1000–1002.
[3] G. D. Enright, K. A. Udachin, I. L Moudrakovski, J. A. Ripmeester, *J. Am. Chem. Soc.* **2003**, *125*, 9896–9897.
[4] J. L. Atwood, L. J. Barbour, A. Jerga, *Angew. Chem.* **2004**, *116*, 3008–3010; *Angew. Chem. Int. Ed.* **2004**, *43*, 2948–2950.
[5] M. I. Ogden, A. L. Rohl, J. D. Gale, *Chem. Commun.* **2001**, 1626–1627.
[6] S. León, D. A. Leigh, F. Zerbetto, *Chem. Eur. J.* **2002**, *8*, 4854–4866.

[7] J. L. Daschbach, P. K. Thallapally, J. L. Atwood, P. McGrail, L. X. Dang, *J. Chem. Phys.* **2007**, *127*, 104703–1–104703–4.
[8] S. Alavi, N. A. Afagh, J. A. Ripmeester, D. L. Thompson, *Chem. Eur. J.* **2006**, *12*, 5231–5237.
[9] K. A. Udachin, I. L. Moudrakovski, C. I. Ratcliffe, J. A. Ripmeester, in preparation.
[10] D. H. Brouwer, I. L. Moudrakovski, K. A. Udachin, G. Enright, J. A. Ripmeester, *Cryst. Growth Des.*, submitted.
[11] W. D. Cornell, P. Cieplak, C. L. Bayly, I. R. Gould, K. M. Merz Jr. , D. M. Ferguson, D. C. Spellmeyer, T. Fox, J. W. Caldwell, P. A. Kollman, *J. Am. Chem. Soc.* **1995**, *117*, 5179–5197. See also, http://amber.scripps.edu
[12] W. F. Wang, *J. Quant. Spectrosc. Radiat. Transfer* **2003**, *76*, 23–30.
[13] J. G. Harris, K. H. Yung, *J. Phys. Chem.* **1995**, *99*, 12021–12024.
[14] R. D. Etters, B. Kuchta, *J. Chem. Phys.* **1989**, *90*, 4537–4541.
[15] S. Nosé, *J. Chem. Phys.* **1984**, *81*, 511–519.
[16] W. G. Hoover, *Phys. Rev. A* **1985**, *31*, 1695–1697.
[17] S. Melchionna, G. Ciccotti, B. L. Holian, *Mol. Phys.* **1993**, *78*, 533–544.
[18] DL_POLY 2.16 (Eds. T. R. Forester, W. Smith), CCLRC, Daresbury Laboratory, **1995**.
[19] D. Frenkel, B. Smit, *Understanding Molecular Simulation, 2nd ed.*, Academic Press, San Diego, **2000**.
[20] M. P. Allen, D. J. Tildesley, *Computer Simulation of Liquids*, Oxford Science Publications, Oxford, **1987**.
[21] P. K. Thallapally, G. O. Llyod, T. B. Wirsig, M. W. Bredenkamp, J. L. Atwood, L. J. Barbour, *Chem. Commun.* **2005**, 5272–5274.
[22] P. K. Thallapally, T. B. Wirsig, L. J. Barbour, J. L. Atwood, *Chem. Commun.* **2005**, 4420–4422.
[23] J. L. Atwood, L. J. Barbour, P. K. Thallapally, T. B. Wirsig, *Chem. Commun.* **2005**, 51–53.
[24] P. K. Thallapally, K. A. Kirby, J. L. Atwood, *New J. Chem.* **2007**, *31*, 628–630.
[25] P. Sozzani, S. Bracco, A. Comotti, L. Ferretti, R. Simonutti, *Angew. Chem.* **2005**, *117*, 1850–1854; *Angew. Chem. Int. Ed. Engl.* **2005**, *44*, 1816–1820.
[26] J. Yang, D. Ma, F. Deng, Q. Luo, M. Zhang, X. Bao, Ch. Ye, *Chem. Commun.* **2002**, 3046–3047.
[27] H. Lee, Y. Seo, Y.-T. Seo, I. L. Moudrakovski, J. A. Ripmeester, *Angew. Chem.* **2003**, *115*, 5202–5205, *Angew. Chem. Int. Ed. Engl.* **2003**, *42*, 5048–5051.
[28] B. F. Graham, J. M. Harrowfield, R. D. Tengrove, A. F. Lagalante, T. J. Bruno, *J. Inclusion Phenom. Macrocyclic Chem.* **2002**, *43*, 179–182.
[29] P. K. Thallapally, L. Dobrzańska, T. R. Gingrich, T. B. Wirsig, L. J. Barbour, J. L. Atwood, *Angew. Chem.* **2006**, *118*, 6656–6659, *Angew. Chem. Int. Ed. Engl.* **2006**, *45*, 6506–6509.

Received: August 27, 2007
Revised: October 19, 2007
Published online: November 30, 2007

